Consider the schematic view of a spectrum density for the interfering signal shown in Figure 23. The schematic in Figure 23 is a simplified version of some of the oscillograms in Section 4. This simplification is for explaining the analysis procedure and it will have no effect on the accuracy of the results. The curve in Figure 23 shows only three peaks of a spectrum. In practice there are more. BW_n in Figure 23 represents bandwidth for the i_{in} peak of the spectrum. The hypothetical spectrum shown in Figure 23 is a good approximation, since it is possible to define BW_n for a section i_{in} of the spectrum over which the power density is approximately linear (4 kHz was assumed to be the smallest subdivision) that there is not restriction on size of BWi.

The interference power under the curve shown in Figure 23 may now be represented by the relation.

$$i_{in} = i_{41} \frac{BW_1}{4000} + i_{42} \frac{BW_2}{4000} + \ldots + i_{4m} \frac{BW_m}{4000}$$

or simply

$$i_{in} = \frac{1}{4000} \sum_{i=1}^{m} i_{4i} \, BW_i \tag{11}$$

Now substitute Equations (11) and (10) into Equation (9):

$$\sum_{i=1}^{m} \frac{i_{4i} BW_i}{n_4 BW_n} \cdot \frac{(npr)_n}{(npr)_i} = \frac{i_c}{n_c} \tag{12}$$

Let i_{4m} represent maximum level of interfering signal and write Equation (12) in the form:

$$\frac{i_{4m}}{n_4} \frac{\sum_{i=1}^{m} i_{4in} BW_i}{BW_n} \cdot \frac{(npr)_n}{(npr)_i} = \frac{i_c}{n_c} \tag{13}$$

where i_{4in} are now the normalized levels of interfering signal. A term-by-term comparison of Equation (13) with Equation (3) indicates:

$$k(\Delta f,m) = \sum_{i=1}^{m} \frac{i_{4in} BW_i}{BW_n} \cdot \frac{(npr)_n}{(npr)_i} \tag{14}$$

The summation term in Equation (14) is smaller than unity. A conservative analysis will result if we let:

$$k = (npr)_n/(npr)_i \tag{15}$$

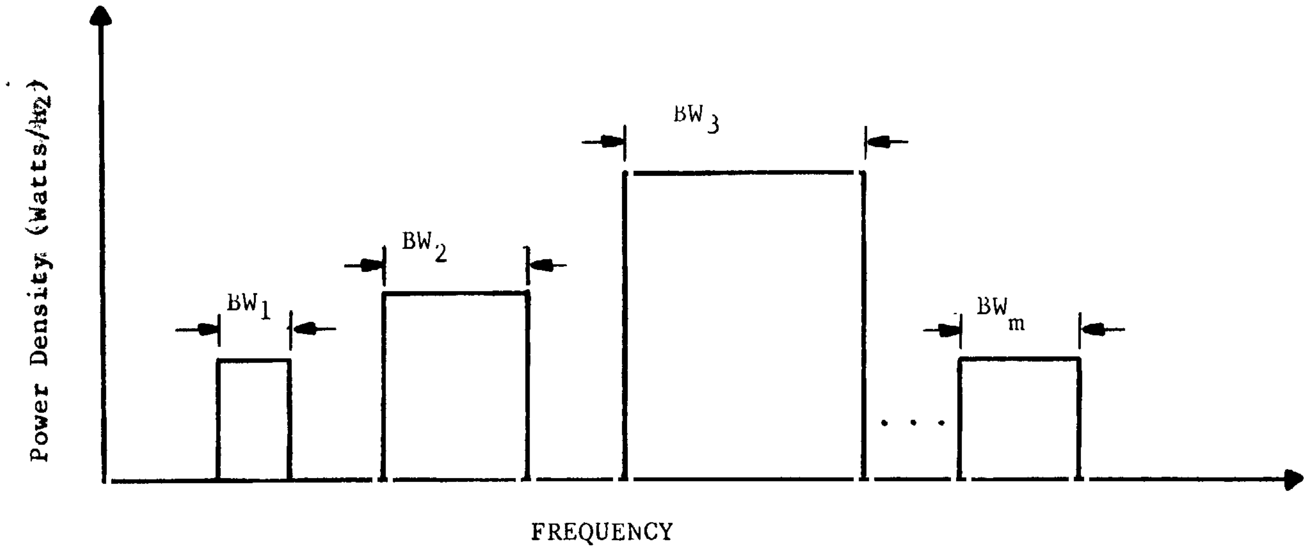

Figure 23: Typical spectrum density for interfering signal.

Substituting Equation (15) into Equation (3) we obtain:

$$\frac{i_4}{n_4} \cdot \frac{(npr)_n}{(npr)_i} \geq \frac{i_c}{n_4} \qquad (16)$$

Therefore

$$k(\Delta f,m) = \alpha_{dB} + (NPR)_n - (NPR)_i \qquad (17)$$

where

$$= \sum_{i=1}^{m} i_{4in} \, BW_i/BW_n$$

The function k for a receiver varies for every channel. For a conservative analysis k was evaluated for a receiver channel which endures the greatest impairment. Evaluation of npr is a key factor in the evaluation of function k which is the desired result.

As was mentioned above npr may be evaluated using closed form expressions for signals using very high or very low modulation indices. For signals with intermediate modulation indices the evaluation of npr should be carried out using the general formula given in Bulletin No. 10-C (Industrial Electronics Ass.):

$$(npr) \sim \frac{2(\delta F)^2 H^2(fr)}{fr^2(f_n - f_1)I} \qquad (18)$$

δF = total multichannel rms deviation
f_r = baseband frequency
f_n = maximum baseband frequency
f_1 = minimum baseband frequency

$$I = \int_{-\infty}^{\infty} [P_1(f+a)P_2(f-a) + P_1(f+b)P_2(f-b)] \, df$$

P_2 (f) = interfering signal power spectra
P_1 (f) = desired signal power spectra

$a = 1/2\ (f_s + f_r)$
$b = 1/2\ (f_s - f_r)$
f_s = frequency separation of desired and interfering signal
$H(f_r)$ = desired signal emphasis function
$= 0.634\ [1 + 1.505\ (f_r/f_n)\ ]$
$H(f_r)$ = 1.0 for unemphasized systems

The approximation given by Equation (18) becomes very good for C/I > 10 dB. A computer program developed by Sharp (1975) for the evaluation of Equation (18) was used to determine $(npr)_i$ and $(npr)_n$. A discussion of the algorithm and the input parameters for the program is given in Sharp's report. This computer model was incorporated in the NTIA computer file. The basic input data consists of emission spectrums (watts/Hz) for the desired and undesired signals and the appropriate parameters associated with these spectrums such as modulation index and bandwidth. For convenience, the computer file has a list of some of the generally used spectrum. This list is called MENUE and the user has the option of selecting a spectrum from this list.

For evaluation of $(NPR)_n$ flat noise was used for function n and in evaluation of $(NPR)_i$ input interference was assumed to be $(\sin x/x)^2$ which is similar to the signal from TDRSS and for a non-TRDSS type signal the interference signal was assumed to be similar to the signal used by Landsat-4 and satellites in SGLS. The calculation was carried out for 48 and 600 channel FDM/FM receivers for f_1 = 12kHz.

The bandwidth for the interference signal (TDRSS signal) was assumed to vary from 2 to 6 MHz. The noise bandwidths were 1 and 20 MHz in the calculation. The modulation indices for the desired signal in the calculations were from 0.1 to 0.5. The simulated FDM/FM signal for these different modulation indices used in the calculations are shown in Figure 24.

Results of the evaluation of function k are given in Figures 25-28. The curves in Figures 25 and 26 show the variation of the function k for different modulation index of the desired signal and when the interference signal is described by $(\sin x/x)^2$. Note that k varies from -0.1 dB for the worst combination to -39 dB depending on the channel number, noise bandwidth, and the bandwidth of the undesired signal. Function k was also evaluated for signals similar to that used by Landsat-4 and the satellites associated with SGLS. This type of signal was referred to as non-TDRSS type signal in Section 4. Figures 27 and 28 show the results of such evaluation when the satellite signal is 256 kbps or 32 kbps, respectively. Note that for these signals values of function k vary from -6 dB to -63 dB.

Interviews with major U.S. manufacturers indicated that terrestrial radio receivers in the 2200-2300 MHz band have generally less than 100 channels and for these receivers the IF bandwidth is approximately 5 MHz. As was discussed earlier, a bandwidth of 2-4 MHz is representative for signals from satellites in the 2025-2300 MHz frequency range. Assuming 5 MHz noise bandwidth for a radio receiver and 4 MHz bandwidth for interfering signal, interpolation of the data shown in Figures 25-28 shows that, for the worst channel k function is approximately equal to -3 dB. For most systems in the 2200-2300 MHz band the value of -3dB is conservative.

ANALYSIS RESULTS

The results of modifications to the GM and NGM programs will now be summarized. Using these results pfd limits for the 2025-2300 MHz frequency range will then be determined. In this frequency range, satellites operate in either geostationary or non-geostationary orbits. The limits for the satellites in the geostationary orbit are different from those in non-geostationary orbit and will be discussed separately. PFD limits given here are applicable to the United States. Assumptions used in their derivation should be reviewed prior to their use by other administrations.

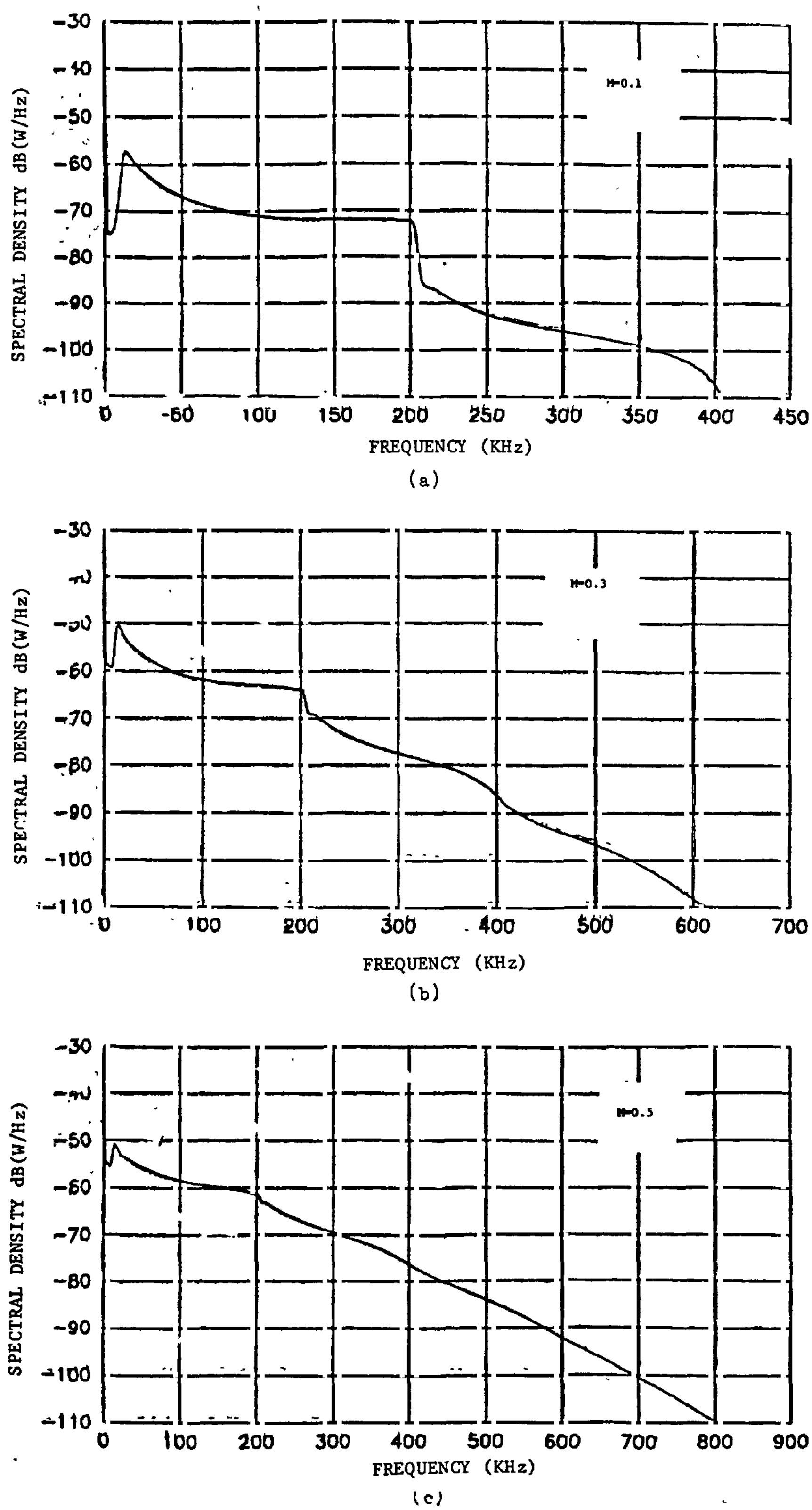

Figure 24. Simulation of FDM/FM signal for 48 channels.
(a) modulation index = 0.1. (b) modulation index = 0.3.
(c) modulation index = 0.5.

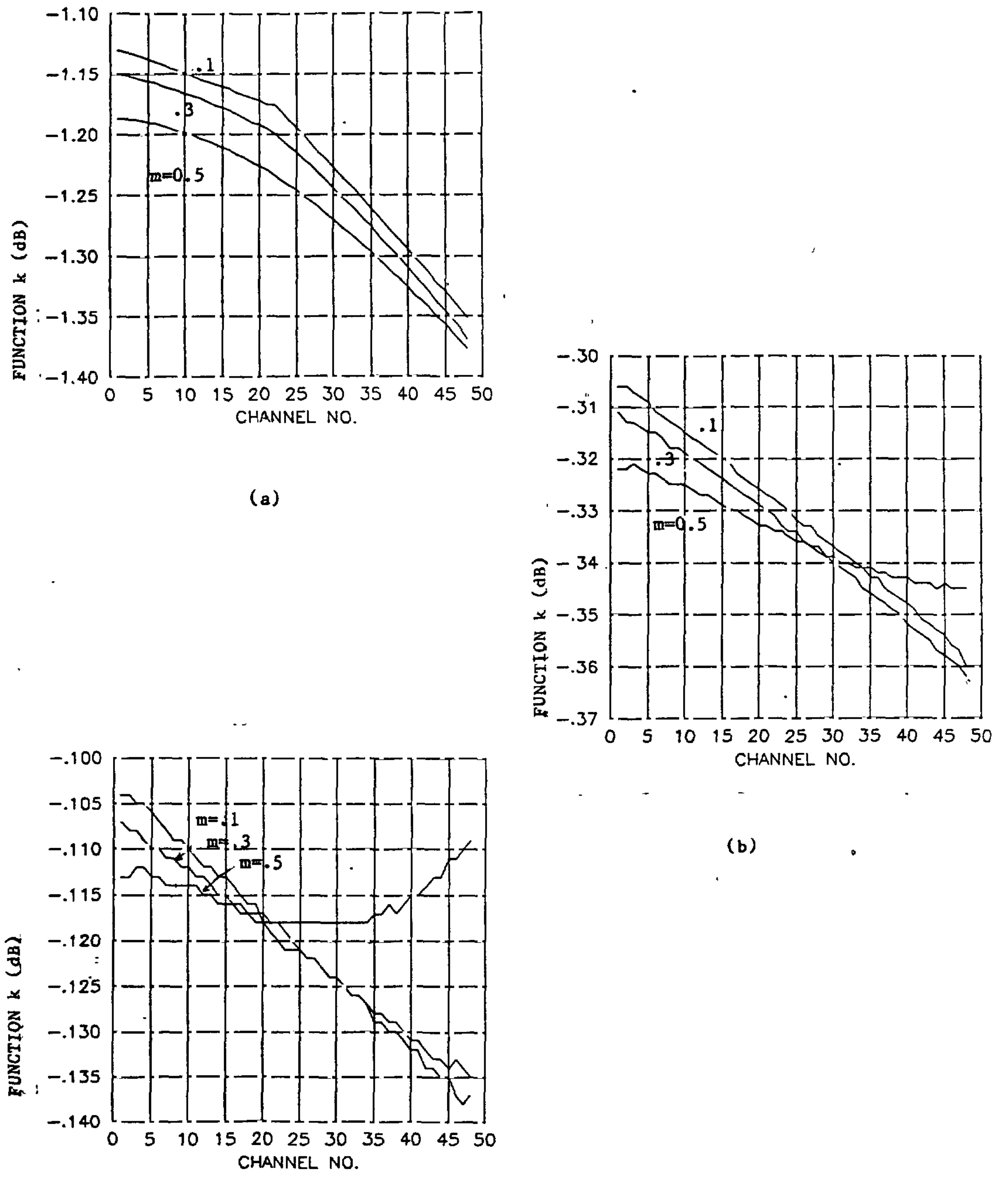

FIGURE 25: A plot of function k vs channel number for TDRSS type-signal and 1 MHz noise bandwidth of receiver: (a) interfering signal bandwidth = 2 MHz, (b) interfering signal bandwidth = 4 MHz; (c) interfering siganl banwidth = 6 MHz.

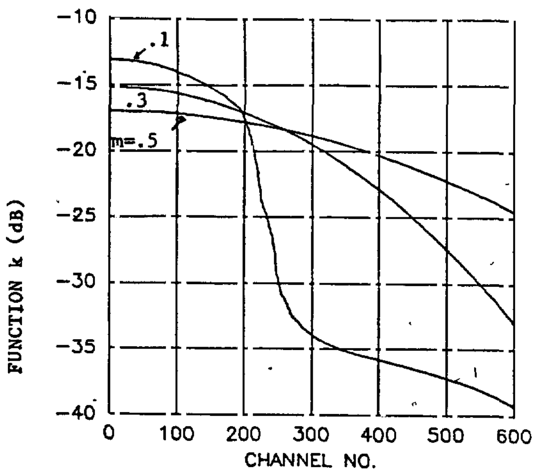

(a)

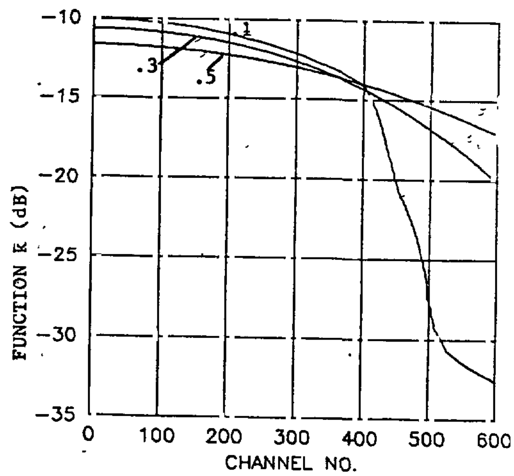

(b)

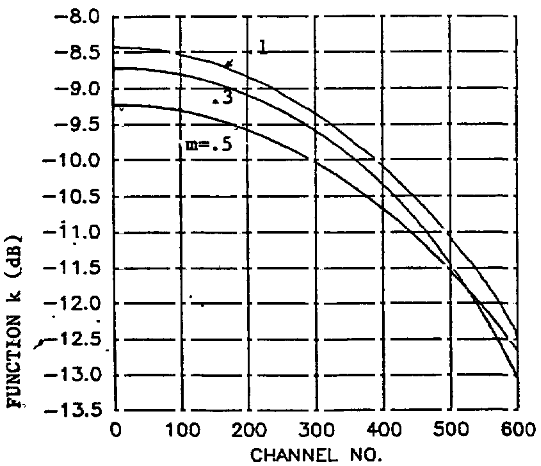

(c)

FIGURE 26: A plot of function k vs channel number for TDRSS-type signal and 20 MHz noise bandwidth of receiver: (a) interfering signal bandwidth = 2 MHz, (b) interfering signal bandwidth = 4 MHz; (c) interfering signal bandwidth = 6 MHz.

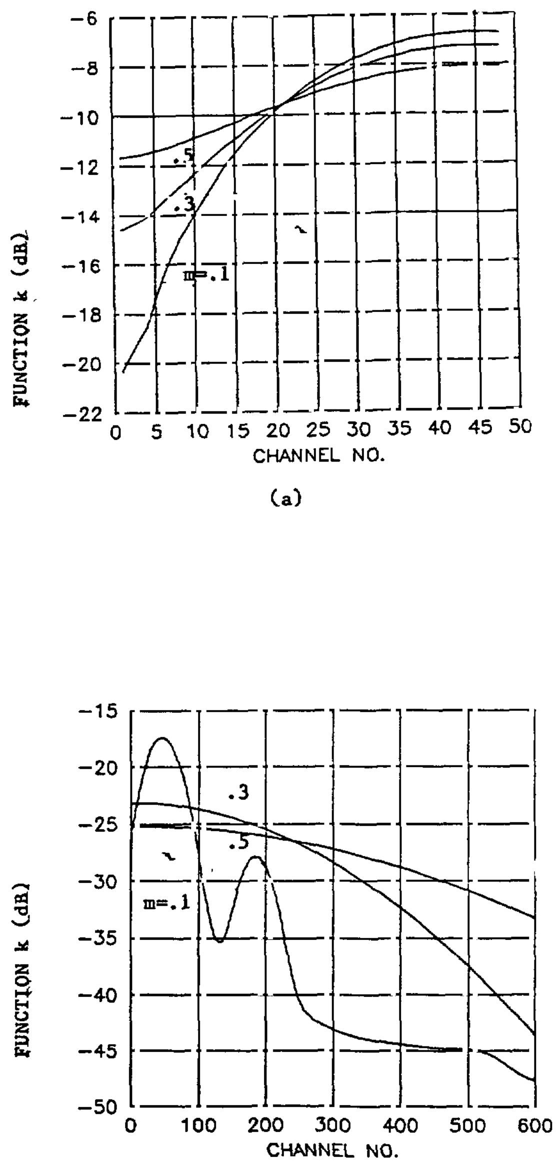

(a)

(b)

FIGURE 27: A plot of function k vs channel number for Landsat-type signal (256 kbps): (a) receiver noise bandwidth equal to 1 MHz, (b) receiver noise bandwidth equal to 20 MHz.

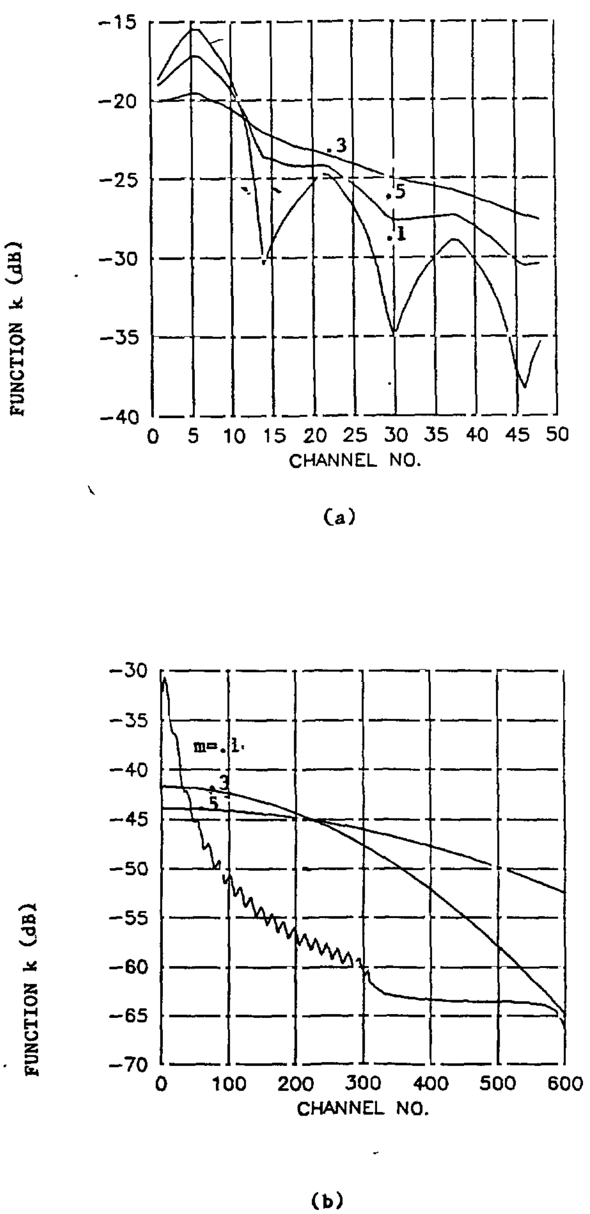

FIGURE 28: A plot of function k vs channel number for Landsat-type signal (32 kbps): (a) receiver noise bandwidth equal to 1 MHz, (b) receiver noise bandwidth equal to 20 MHz.

Modifications to GM and NGM Computer Models

Modifications to the GM and NGM computer models were discussed above and the effects of each modification on pfd limits were separately calculated. The modifications which proved to have significant impact on the pfd limits for the geostationary orbit were those due to the frequency engineering of trendline and receiver transfer function. The multiple-orbit effects and latter two modifications also showed a sizeable effect on the pfd limits for the satellites in the non-geostationary orbits. Fading statistics based on the data obtained in several regions in the United States indicated a negligible change in the pfd limits compared with originally calculated limits using the data obtained in Europe and given in CCIR Report 338-3. Similarly the inclusion of the fading statistics in the GM computer model, although improving the consistency of the approach used in the two models, did not change the value of the pfd limits which were evaluated without fading statistics.

pfd Limits for Satellites in Geostationary Orbit

Considering the modifications due to the frequency engineering of a trendline and the data representative of the characteristics of the systems in terrestrial services given in Section 4, the calculated pfd limit for the satellites in geostationary orbit may be summarized as shown in Table 9. The data in Table 9 does not include 3 dB correction due to the receiver transfer function.

The results corresponding to a 15 degree satellite spacing and double frequency engineering of a trendline shown in Table 9 are realistic for the satellite operations in the 2025-2300 MHz frequency range. Fifteen-degree separation corresponds to approximately 13 satellites in the geostationary orbit. According to the data in Section 4, there are approximately 13 satellites presently in operation in the geostationary orbit. This is highly conservative, since it is difficult to envision that all 13 satellites will operate co-channel with the terrestrial receivers in a trendline. In addition, double frequency engineering is a technique rarely used in a long-haul communication. A four-frequency plan is favored more by commercial communication industries. However, this conservative choice of parameters should compensate for any future growth in the number of satellites and will protect the rare occasions where terrestrial radio users use two frequency plans. The United States are bounded by 20 to 50 degree latitudes. The relaxation in the present pfd indicated by the entries in Table 9 ranges from 6.5 to 11.9 dB for double frequency plan and spacing between satellites in the range of 10 to 20 degrees. Adding 3dB correction factor due to the receiver transfer function the calculated values for relation of pfd vary from 9.5 to 14.9. A 10 dB relaxation in the present pfd limits was found to be reasonable. Therefore, the minimum value for pfd limit in the 2025-2300 MHz frequency range may be determined to be -144 dB (W/m^2) in any 4 kHz frequency band based on the results given in Table 9. This new limit indicates approximately 10dB increase, including 3 dB correction for the receiver transfunction discussed before, from the existing limits. This pfd limit was calculated using the information on the spectrum usage in the United States.

TABLE 9

CHANGE IN pfd LIMITS, dB (W/m^2) IN ANY 4 kHz, FOR SATELLITES IN GEOSTATIONARY ORBIT

FREQUENCY PLAN	LATITUDE (deg)	SATELLITE SPACING (deg)			
		3	10	15	20
Single	20	0.0	4.5	8.8	8.9
Single	30	0.0	3.6	8.6	8.7
Single	40	0.0	3.4	8.0	8.3
Single	50	0.0	3.3	6.5	8.1
Double	20	1.5	8.4	11.7	11.9
Double	30	1.2	8.0	11.7	11.8
Double	40	1.0	7.4	11.0	11.2
Double	50	0.0	6.5	9.2	11.5
Four	20	4.5	11.9	14.4	14.5
Four	30	3.8	8.8	14.3	14.4
Four	40	3.7	8.5	14.1	14.3
Four	50	2.2	8.2	12.8	14.2

pfd Limits for Satellites in Non-Geostationary Orbits

It was shown earlier that the effects of interference from satellites in non-geostationary orbits are independent of those from satellites in geostationary orbit. Hence, the modified NGM computer model was used to evaluate the pfd limits for satellites in non-geostationary orbits. The effects on the pfd limits after a number of modifications to the NGM program were discussed previously in this section. Of these modifications frequency engineering of a trendline, receiver transfer function, and multi-orbit effects have significant impact on pfd limits in the 2025-2300 MHz frequency range.

The data in Section 4 were used in conjunction with the modified NGM simulation model to calculate the pfd limits for low-orbit satellites in the 2025-2300 MHz frequency range. The results of the calculations for single, double, and four-frequency plan of radio-relay trendlines are given in Figures 29, 30, and 31 respectively. The data in Figures 29-31 show the cumulative interference power level as a function of time at the input to receivers in a typical trendline in the 2025-2300 MHz frequency range. Curve E in Figures 29-30 show the criteria for noise due to interference in the hypothetical reference circuit established by the CCIR Recommendation 357-3 (1978). Note that the interference Curve B in Figures 29-31 differs from the criteria Curve E by 10, 13, and 16 dB for single, double, and four-frequency plan, respectively. The interference curves in these figures do not include the 3 dB correction due to the receiver transfer function discussed earlier. The case of double-frequency plan is of interest. A 13 dB increase to the interference in curve on Figure 30 will allow the noise due to interference to reach the noise criteria level accepted by the CCIR. Therefore, the pfd limit for the satellites in non-geostationary orbits may be increased by 16 dB without exceeding the noise criteria level set by the CCIR in the frequency range 2025-2300 MHz. The minimum pfd limits for non-geostationary satellites may then be increased to -138 dBW/m^2 in any 4 kHz bandwidth. The calculated pfd limits using modified NGM computer model are given in Figure 32.

Note that the shape of the curve in Figure 32 is not different from that originally recommended by the ITU Radio Regulations. The data in Figure 32 were obtained using spectrum usage data in the United States.

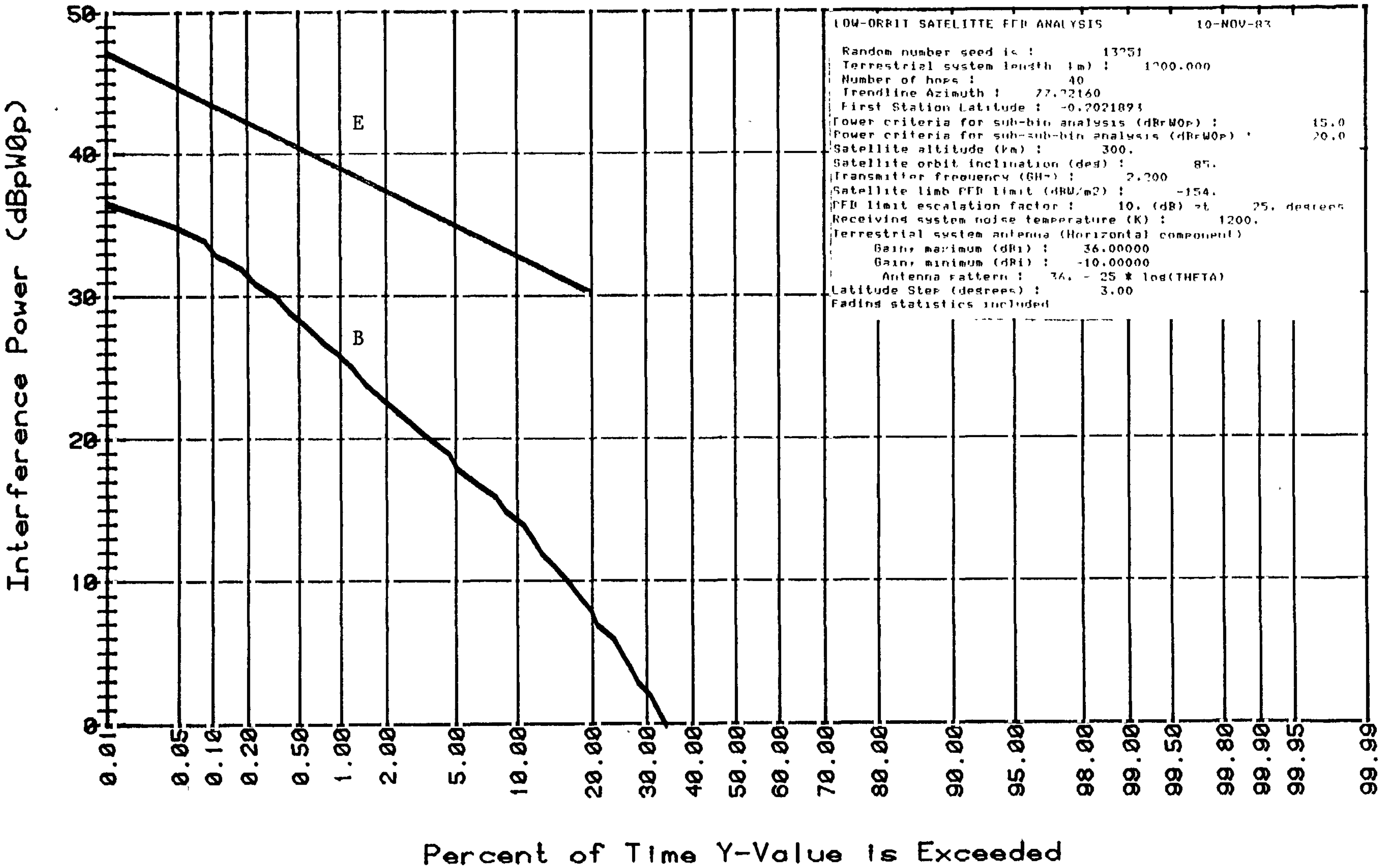

Figure 29 Interference Power From Eight Satellites in Non-Geostationary Orbits to Radio-Relay Receivers in a Trendline Using Single Frequency Plan.

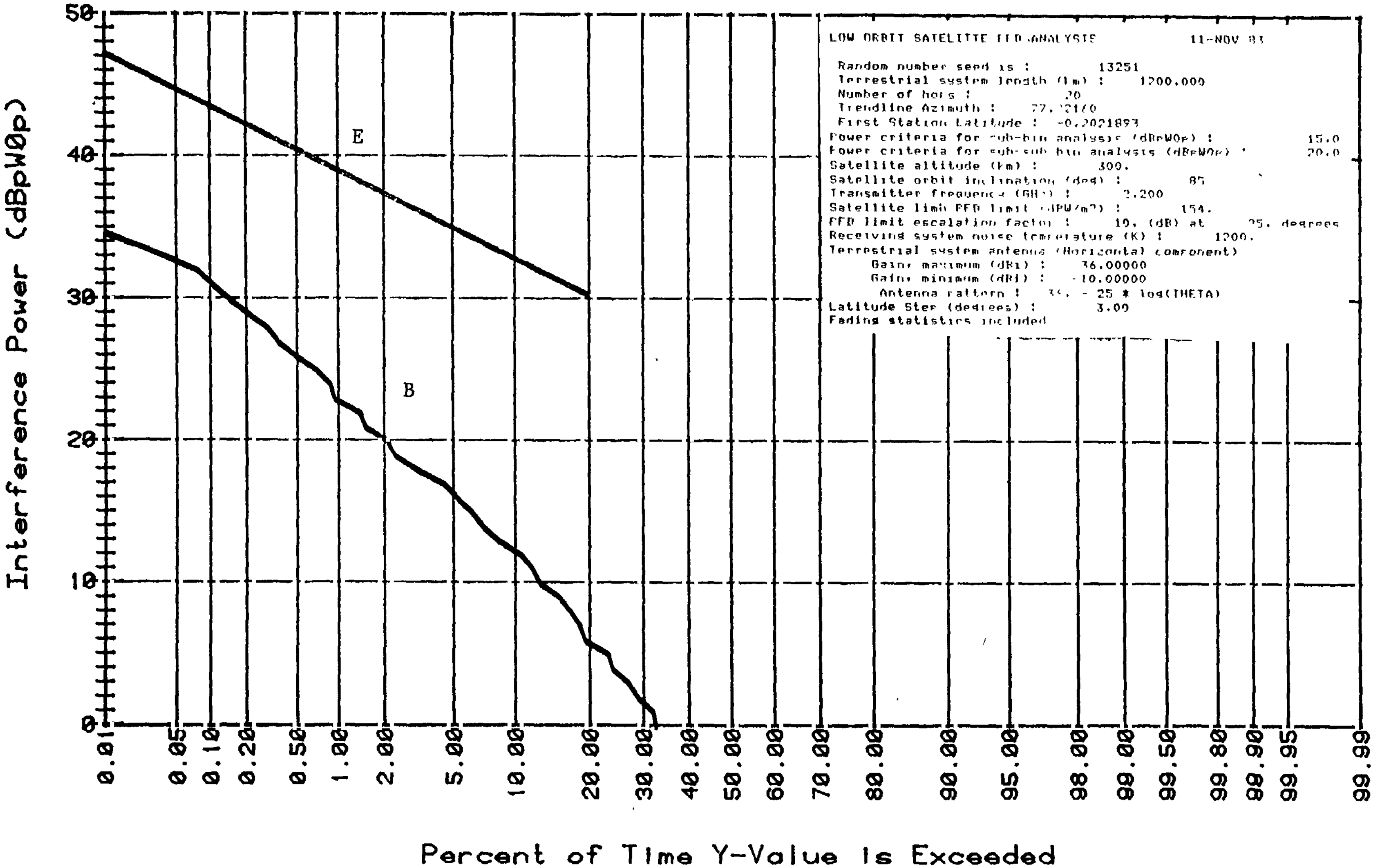

Figure 30 Interference Power From Eight Satelllites in Non-Geostationary Orbits to Radio-Relay Receivers in a Trendline Using Double Frequency Plan

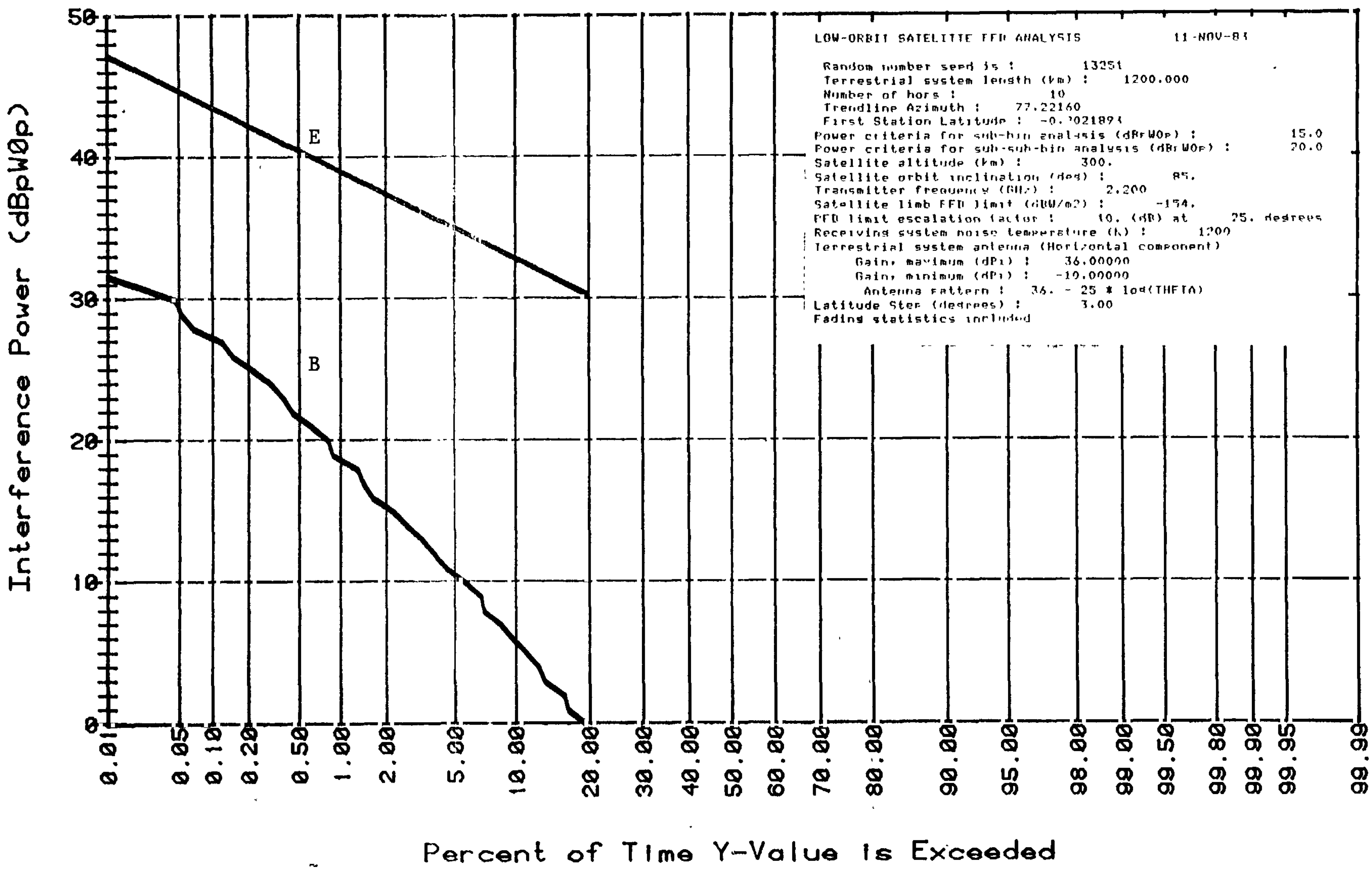

Figure 31 Interference Power from Eight Satellites in Non-Geostationary Orbits to Radio-Relay Receivers in a Trendline Uisng Frou Frequency Plan.

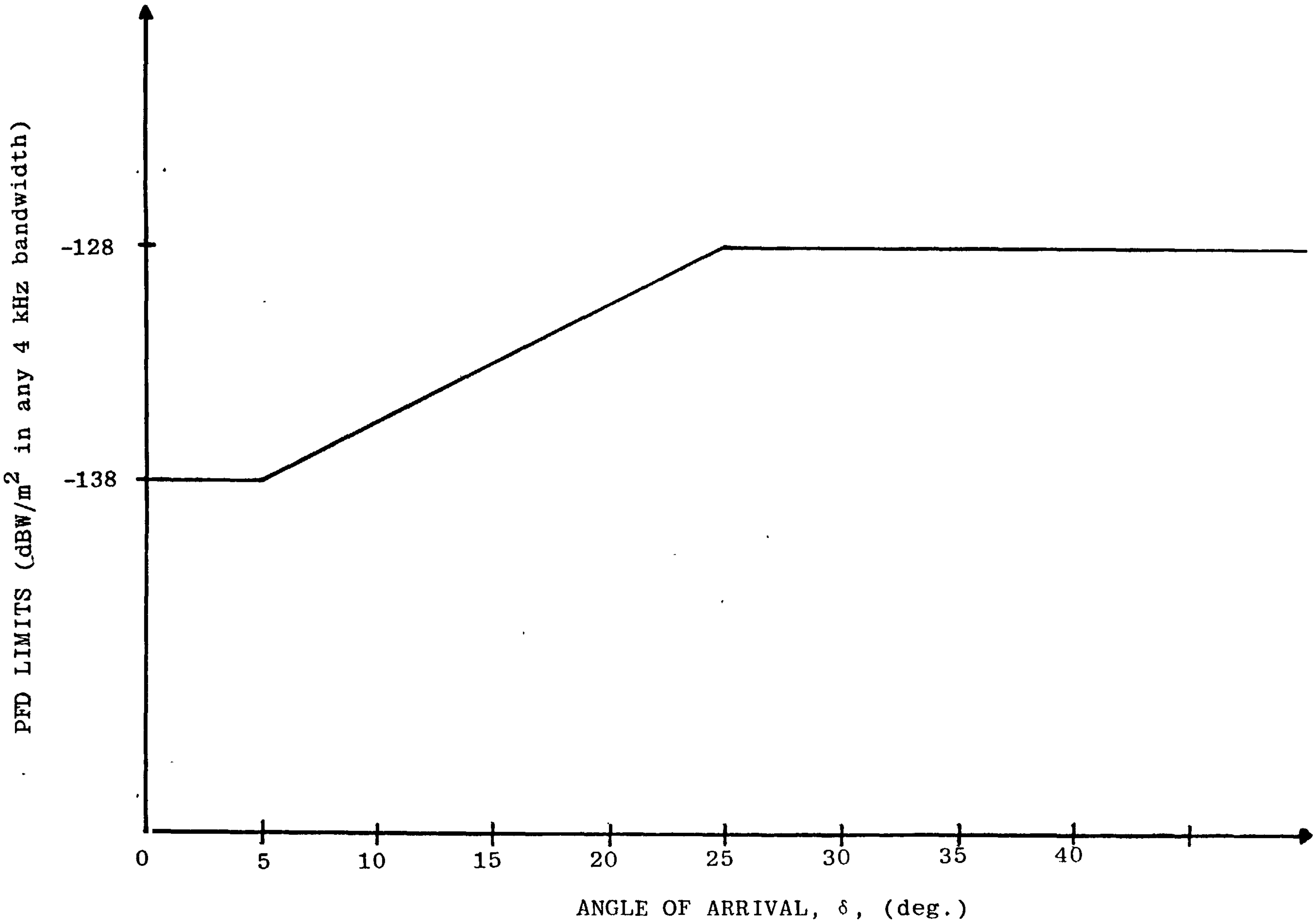

Figure 32 pfd Limits for Satellites in Non-Geostationary Orbits